

University of Groningen

N-Type Organic Thermoelectrics of Donor-Acceptor Copolymers

Liu, Jian; Ye, Gang; van der Zee, Bas; Dong, Jingjin; Qiu, Xinkai; Liu, Yuru; Portale, Giuseppe; Chiechi, Ryan C.; Koster, L. Jan Anton

Published in:
Advanced materials

DOI:
[10.1002/adma.201804290](https://doi.org/10.1002/adma.201804290)

IMPORTANT NOTE: You are advised to consult the publisher's version (publisher's PDF) if you wish to cite from it. Please check the document version below.

Document Version
Publisher's PDF, also known as Version of record

Publication date:
2018

[Link to publication in University of Groningen/UMCG research database](#)

Citation for published version (APA):

Liu, J., Ye, G., van der Zee, B., Dong, J., Qiu, X., Liu, Y., Portale, G., Chiechi, R. C., & Koster, L. J. A. (2018). N-Type Organic Thermoelectrics of Donor-Acceptor Copolymers: Improved Power Factor by Molecular Tailoring of the Density of States. *Advanced materials*, 30(44), [1804290]. <https://doi.org/10.1002/adma.201804290>

Copyright

Other than for strictly personal use, it is not permitted to download or to forward/distribute the text or part of it without the consent of the author(s) and/or copyright holder(s), unless the work is under an open content license (like Creative Commons).

The publication may also be distributed here under the terms of Article 25fa of the Dutch Copyright Act, indicated by the "Taverne" license. More information can be found on the University of Groningen website: <https://www.rug.nl/library/open-access/self-archiving-pure/taverne-amendment>.

Take-down policy

If you believe that this document breaches copyright please contact us providing details, and we will remove access to the work immediately and investigate your claim.

Downloaded from the University of Groningen/UMCG research database (Pure): <http://www.rug.nl/research/portal>. For technical reasons the number of authors shown on this cover page is limited to 10 maximum.

N-Type Organic Thermoelectrics of Donor–Acceptor Copolymers: Improved Power Factor by Molecular Tailoring of the Density of States

Jian Liu,* Gang Ye, Bas van der Zee, Jingjin Dong, Xinkai Qiu, Yuru Liu, Giuseppe Portale, Ryan C. Chiechi, and L. Jan Anton Koster*

It is demonstrated that the n-type thermoelectric performance of donor–acceptor (D–A) copolymers can be enhanced by a factor of >1000 by tailoring the density of states (DOS). The DOS distribution is tailored by embedding sp²-nitrogen atoms into the donor moiety of the D–A backbone. Consequently, an electrical conductivity of 1.8 S cm⁻¹ and a power factor of 4.5 μW m⁻¹ K⁻² are achieved. Interestingly, an unusual sign switching (from negative to positive) of the Seebeck coefficient of the unmodified D–A copolymer at moderately high dopant loading is observed. A direct measurement of the DOS shows that the DOS distributions become less broad upon modifying the backbone in both pristine and doped states. Additionally, doping-induced charge transfer complexes (CTC) states, which are energetically located below the neutral band, are observed in DOS of the doped unmodified D–A copolymer. It is proposed that charge transport through these CTC states is responsible for the positive Seebeck coefficients in this n-doped system. This is supported by numerical simulation and temperature dependence of Seebeck coefficient. The work provides a unique insight into the fundamental understanding of molecular doping and sheds light on designing efficient n-type OTE materials from a perspective of tailoring the DOS.

light-emitting diodes, organic/hybrid solar cells, organic thermoelectrics (OTE), and field-effect transistor etc.^[1–14] Although this strategy is widely utilized in academic and industrial fields, the doping process is still little understood. So far, two different models have been proposed to describe the molecular doping of OSCs: the integer charge transfer (ICT) model and the molecular orbital hybridization (MOH) model.^[1,2,15,16] Both of them consider the molecular doping as a two-step process: charge transfer followed by charge carrier release. In the ICT model, an ICT between donor and acceptor is assumed. In the MOH model, frontier orbital hybridization yields a new state from which charge carriers can be released. These charge transfer processes give rise to charge transfer complexes (CTC).^[16,17] In the ICT model, these CTCs are regarded to be energetically located below/above the center of the lowest unoccupied molecular orbital (LUMO)/highest occupied molecular


Molecular doping of organic semiconductors (OSCs) has proven a powerful strategy to modulate the electronic properties for advancing the development of organic electronics, such as

orbital (HOMO) levels by an energy difference (ΔE) of several 100 meV due to a large Coulomb force from the ionized dopant molecules.^[16,18] As a next step, free charge carriers are released from those CTC states by thermal ionization. Such a two-step process explains the typically low doping efficiency and freeze-out of free charge carriers in a doped OSC.^[1,16] Regardless the model, the molecular doping process can be regarded as a modification of the density of states (DOS) of the OSC upon dopant admixture. As the DOS is closely related to the electronic properties of OSCs, a better understanding of the molecular doping and its relation to the DOS is urgently required.

In the category of OTE, the molecular doping is usually employed to control the carrier density in OSCs to achieve high power factors ($S^2\sigma$, where S and σ are Seebeck coefficient and electrical conductivity, respectively).^[19,20] For the practical TE applications, both efficient p-type and n-type TE materials are required; however, the development of the latter lags much behind that of the former.^[19,21–23] For this reason, growing research efforts are being directed towards developing better n-type TE materials.^[24–27] So far, advanced conjugated-backbone designs targeting favorable energetics, high mobility, planar structure, and good host/dopant miscibility

Dr. J. Liu, G. Ye, B. van der Zee, J. Dong, X. Qiu, Y. Liu, Dr. G. Portale, Prof. R. C. Chiechi, Prof. L. J. A. Koster
Zernike Institute for Advanced Materials
University of Groningen
Nijenborgh 4, NL-9747 AG, Groningen, The Netherlands
E-mail: jian.liu@rug.nl; l.j.a.koster@rug.nl

G. Ye, X. Qiu, Y. Liu, Prof. R. C. Chiechi
Stratingh Institute for Chemistry
University of Groningen
Nijenborgh 4, NL-9747 AG, Groningen, The Netherlands

 The ORCID identification number(s) of the author(s) of this article can be found under <https://doi.org/10.1002/adma.201804290>.

© 2018 The Authors. Published by WILEY-VCH Verlag GmbH & Co. KGaA, Weinheim. This is an open access article under the terms of the Creative Commons Attribution-NonCommercial-NoDerivs License, which permits use and distribution in any medium, provided the original work is properly cited, the use is non-commercial and no modifications or adaptations are made.

DOI: 10.1002/adma.201804290

have been reported.^[8,23,28–33] Moreover, donor–acceptor (D–A) copolymers can show very high charge carrier mobilities.^[34,35] The first trial based on D–A copolymer is doping poly{[N,N'-bis(2-octyldodecyl)-naphthalene-1,4,5,8-bis(dicarboximide)-2,6-diyl] (NDI)-alt-5,5'-(2,2'-bithiophene)} (2T) (N2200) with (4-(1,3-dimethyl-2,3-dihydro-1H-benzoimidazol-2-yl)phenyl) dimethylamine (n-DMBI).^[36] As a result, electrical conductivities in the range of 1×10^{-3} – 5×10^{-3} S cm⁻¹ were achieved.^[36,37] Recent works demonstrated that the doping of D–A copolymers can be enhanced by increasing the host/dopant miscibility through the use of polar side chains.^[28,38] This can achieve an optimized electrical conductivity of up to 0.3 S cm⁻¹.^[28] However, the electrical conductivity of the n-doped D–A copolymer is still at a low level, which causes a relatively low power factor of $\approx 0.4 \mu\text{W m}^{-1} \text{K}^{-2}$. As is well known, increasing the carrier density by molecular doping enables an increase in electrical conductivity, but usually at the cost of the reducing Seebeck coefficient. Therefore, an alternative strategy is desired for simultaneous increase in the two TE parameters. Fundamentally, the Seebeck coefficient and electrical conductivity can be described as^[39]:

$$S = -\frac{k}{q} \int \left(\frac{E - E_F}{kT} \right) \frac{\sigma(E)}{\sigma} dE \quad (1)$$

where $\sigma(E)$, T , k , and q are conductivity distribution function, absolute temperature, Boltzmann constant, and elementary charge, respectively. From equation (1), it is clear that both the electrical conductivity and the Seebeck coefficient are closely related to the DOS distribution. Recently, Kemerink et al., broadened the DOS distribution by mixing two donor

polymers in order to obtain very high Seebeck coefficients (of over 1 mV K⁻¹) at the expense of electrical conductivity.^[40] To the best of our knowledge, none of the previous works focused on improving the n-type OTE from a perspective of DOS.

Here, we demonstrate that the n-type thermoelectric properties of D–A copolymers can be greatly improved by tailoring the DOS. The tailoring of the DOS is realized by introducing sp²-nitrogen (N) into the donor moiety of an NDI-2T backbone, which improves not only the molecular planarity but also the structural order. Consequently, a very high electrical conductivity of 1.8 S cm⁻¹ for doped D–A copolymers is achieved. Interestingly, we observed an unusual sign switching of the Seebeck coefficient from negative to positive with increasing the dopant loading in the D–A copolymer without sp²-nitrogen atoms into the donor moiety. A direct DOS profile measurement indicates that the DOS distributions become narrower after backbone modification in both the pristine and doped state. Additionally, doping-induced CTC, which are energetically located below the neutral band, were observed for the doped unmodified D–A copolymer. We propose that charge transport through these CTC states is responsible for the positive Seebeck coefficient in this n-doped system, which is supported by numerical simulation and the temperature dependence of the Seebeck coefficient. We argue that tailoring the DOS of a doped film towards reducing those CTC states within the bandgap can increase the absolute Seebeck coefficient. Therefore, a very good power factor of $4.5 \pm 0.2 \mu\text{W m}^{-1} \text{K}^{-2}$ for n-doped D–A copolymers is achieved in the doped modified copolymer.

Figure 1a shows the chemical structures of two D–A copolymers, which are denoted as PNDI2TEG-2T and PNDI2TEG-2Tz,

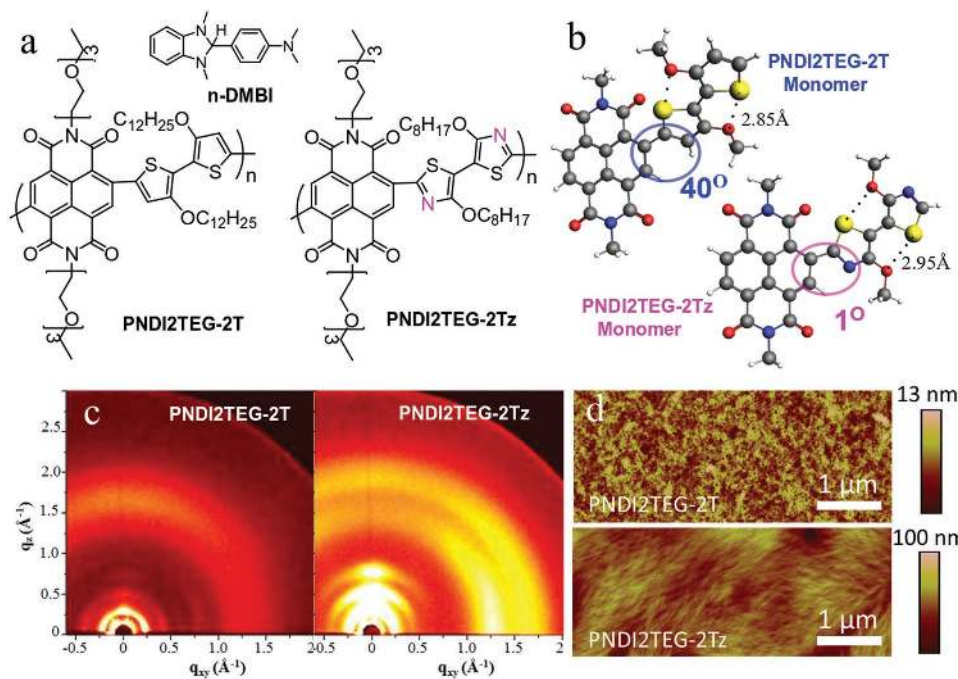


Figure 1. a) The chemical structures of PNDI2TEG-2T, PNDI2TEG-2Tz, and n-DMBI; b) DFT-optimized geometries for PNDI2TEG-2T repeat unit and PNDI2TEG-2Tz repeat unit. Alkyl and N-ethylene glycol substituents are replaced by methyl groups to simplify the calculations. Calculations were carried out at the B3LYP/6-31G** level. The dihedral angles and the regions of steric repulsion torsion are indicated by the circles; c) 2D GIWAXS patterns of the pristine PNDI2TEG-2T and PNDI2TEG-2Tz thin films; and d) AFM images of pristine PNDI2TEG-2T and PNDI2TEG-2Tz films.

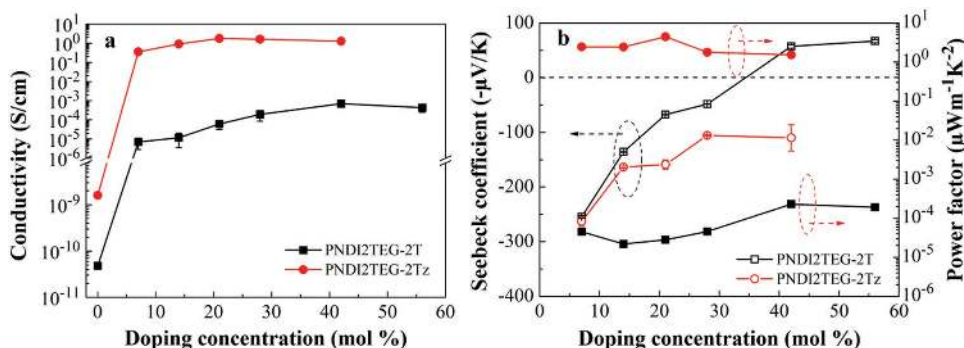


Figure 2. a) The electrical conductivities and b) Seebeck coefficient and power factor of pristine and doped PNDI2TEG-2T and PNDI2TEG-2Tz thin films.

respectively. The synthetic routines are demonstrated in the Supporting Information. Both of them use NDI as the acceptor moiety, which carries the polar triethylene glycol side chains to enable good host/dopant miscibility. PNDI2TEG-2T was synthesized by copolymerizing NDI monomers with electron-rich bithiophene (2T) monomers. With sp²-nitrogen atoms embedded in the 2T units, PNDI2TEG-2Tz was obtained with bithiazole (2Tz) as the donor moiety. Density functional theory (DFT) calculations were carried out for the monomers of the two D–A copolymers as shown in Figure 1b. The computed S···O distance is only 2.85 and 2.95 Å for the PNDI2TEG-2T and the PNDI2TEG-2Tz monomers, respectively. These distances are significantly smaller than the sum of S and O van der Waals radii (3.32 Å), strongly suggesting that the backbones are planar in the solid state. However, the energy-minimized dihedral angle between the plane of the NDI block with neighboring arene units are distinctly different. The dihedral angle between the NDI block and bithiophene blocks is 40° in PNDI2TEG-2T, while the PNDI2TEG-2Tz exhibits a dihedral angle of only 1°. These results indicate an improved molecular planarity after introducing sp²-N atoms, which is consistent with previous reports.^[41,42]

Figure 1c displays the two-dimensional (2D) grazing incidence wide angle X-ray scattering (GIWAXS) patterns of the pristine PNDI2TEG-2T and PNDI2TEG-2Tz thin films. Clearly, PNDI2TEG-2T chain preferentially packs in a ‘face-on’ orientation, in agreement with the literature,^[43] as evidenced by the orientation of the (100) reflection along the horizontal q_y direction. On the contrary, PNDI2TEG-2Tz chain stacks edge-on relative to substrate, (100) reflection along the vertical q_z direction. Both copolymers exhibit q_{xy} (010) reflection at 1.4 Å⁻¹, associated with a π - π stacking distance of \approx 4.0 Å. It is very important to note that, PNDI2TEG-2Tz shows an extra peak at around 1.75 Å⁻¹ (3.6 Å) likely belonging to the π - π stacking of thiazole moiety.^[44] The doping process appears not to significantly change the molecular orientations of the two polymers, having an influence only on the extent of developed crystallinity (Figure S5, Supporting Information).

The cyclic voltammetry characterization of PNDI2TEG-2T and PNDI2TEG-2Tz was carried out to investigate the effects of backbone modification on the energetics (see Figure S6, Supporting Information). This characterization confirms that the effect of the polar side chains (as compared to alkyl ones) on energetics is small (see Figure S6, Supporting Information),

in accordance with our previous findings.^[38] The introduction of the electron-deficient sp²-nitrogen atoms causes a shift of LUMO/HOMO level from -4.18/-5.39 eV for PNDI2TEG-2T to -4.26/-5.56 eV for PNDI2TEG-2Tz, which is consistent with the DFT calculation (Figure S7, Supporting Information).

Previous works showed n-DMBI is a good n-type dopant for NDI-based copolymers.^[28,36,38] Therefore, n-DMBI was also employed to dope the two D–A copolymers in the present study. Figure 1d shows surface morphologies of pristine D–A copolymers characterized by atomic force microscopy (AFM). PNDI2TEG-2Tz exhibits a fibril-textured morphology, which is not apparently seen for PNDI2TEG-2T. This indicates an improved molecular self-assembling after backbone modification and agrees well with the molecular conformation and GIWAXS data. The effects of doping on the surface morphology were also investigated (see Figures S8 and S9, Supporting Information). Both doped D–A copolymers show good surface morphology with few aggregates. These results indicate good host/dopant miscibilities for both doped D–A copolymers, which are likely enabled by their polar side chains and may guarantee efficient n-doping for both D–A copolymers.

Figure 2a displays the electrical conductivity (σ) of the pristine and doped PNDI2TEG-2T and PNDI2TEG-2Tz thin films at different doping concentrations (see Figure S10 in the Supporting Information for the current–voltage data). The pristine PNDI2TEG-2T and PNDI2TEG-2Tz films show very low electrical conductivities of 4.8×10^{-11} and 1.6×10^{-9} S cm⁻¹, respectively. Upon molecular doping with n-DMBI, the PNDI2TEG-2T based film exhibits an optimized conductivity of 7.0×10^{-4} S cm⁻¹ at a doping concentration of 42 mol%. An optimized σ of 1.8 S cm⁻¹ is obtained for the doped PNDI2TEG-2Tz at a doping concentration of 21%, which represents an enhancement of more than a factor of 2000 relative to that of the doped PNDI2TEG-2T film and a new record for n-doped D–A copolymers. Our results indicate that the backbone modification by embedding sp²-nitrogen atoms in the donor moiety is a way to tune the charging behavior of D–A copolymers.

Figure 2b displays the Seebeck coefficients of differently doped D–A copolymers (see Figures S10 and S11, Supporting Information). At a doping concentration of 7 mol%, the doped PNDI2TEG-2T and doped PNDI2TEG-2Tz films exhibit very similar Seebeck coefficients of -254.5 ± 2.5 and -263.1 ± 8.7 μ V K⁻¹, respectively. The negative sign of Seebeck coefficient

Table 1. Thermoelectric properties of solution-processed n-type conjugated polymers.

Material	D–A type	Conductivity [S cm ⁻¹]	Seebeck coefficient [μVK ⁻¹]	Power factor [μW m ⁻¹ K ⁻²]	Reference
PNDI2TEG-2T	Yes	7.0 × 10 ⁻⁴	57.2 ± 3.1	2.3 × 10 ⁻⁴	This work
PNDI2TEG-2Tz	Yes	1.8 ± 0.1	-159 ± 8	4.6 ± 0.2	This work
N2200	Yes	8 × 10 ⁻³	-850	0.6	[36]
TEG-N2200	Yes	0.17	-153	0.4	[38]
p(gNDI-gT2)	Yes	0.3	-93	0.4	[28]
P(BTP-DPP)	Yes	0.45	-	-	[30]
P(NDI2OD-Tz2)	Yes	0.06	-447	1.5	[33]
BBL	No	1.2	-60	0.43	[8]
FBDPPV	No	14	-140	28	[31]
CIBDPPV	No	0.62	-99 ± 9	0.63	[29]
PNDTI-BBT- DP	No	5	-169	14	[24]

indicates n-type doping with electrons as the dominating charge carriers. By increasing the doping concentration up to 28 mol%, the Seebeck coefficients of the doped PNDI2TEG-2T and PNDI2TEG-2Tz films are gradually changed to -48.4 ± 0.3 and $-105.7 \pm 1.1 \mu\text{V K}^{-1}$, respectively. The doped PNDI2TEG-2T films show negligible power factors on an order of magnitude of $\approx 10^{-5} \mu\text{W m}^{-1} \text{K}^{-2}$; while n-doping of PNDI2TEG-2Tz gives a maximum power factor of $4.5 \pm 0.2 \mu\text{W m}^{-1} \text{K}^{-2}$ at a doping concentration of 21 mol%, which is the best result reported by far for n-doped D–A copolymers (see Table 1). These results confirm the effectiveness of tailoring the donor moiety for promoting thermoelectric performance of n-type D–A copolymers. Interestingly, by further increasing the doping concentration, we observed an unusual sign switching for the Seebeck coefficient in the doped PNDI2TEG-2T system, which displays positive Seebeck coefficients of 57.2 ± 3.1 and $66.8 \pm 2.7 \mu\text{V K}^{-1}$ at doping concentrations of 42% and 56 mol%, respectively. It is noted that the possibility of the positive Seebeck coefficient originating from the movement of the ionized dopant can be excluded here as we used a steady-state method for the Seebeck coefficient measurement.^[45] The Seebeck coefficient is determined by the difference between the Fermi level energy (E_F) and the charge transport energy (E_T).^[44] Hwang et al. reported a change of sign of the Seebeck coefficient upon doping by chemically n-doping poly(pyridinium phenylene) (P(PymPh)) with a very strong reductant.^[46] As a result of intense doping, the E_F continuously passes over the original LUMO level of P(PymPh), which is sufficiently filled up by the extrinsic electrons and acts as the new HOMO with the former LUMO+1 effectively becoming the new LUMO.^[46] They considered this transition in electronic states by extremely strong doping with a doping level of > 1 as the main cause of the sign switching of Seebeck coefficient.^[46] However, we wish to point out that the change of sign in our system occurs at a much lower doping level.

To gain insight in the doping processes of the D–A copolymers, we measured the UV–vis–NIR absorption spectra of pristine and doped PNDI2TEG-2T and PNDI2TEG-2Tz thin films (see Figure 3a and 3b). The pristine PNDI2TEG-2T film shows two characteristic neutral features centered at 403 and 843 nm, which we assign to the π – π^* transition and an intramolecular

charge-transfer band, respectively.^[8,37] Similarly, two neutral peaks at 465 and 907 nm were observed in the pristine PNDI2TEG-2Tz film. As the D–A copolymers are doped with more n-DMBI, the transitions in the neutral spectra peaks gradually decrease in intensity in the two doped systems. This is accompanied by the appearance of additional absorption bands at 570 and 975 nm for the doped PNDI2TEG-2T and at 1000 nm for the doped PNDI2TEG-2Tz, respectively. Another low-energy broad absorption in the range of 1800–2500 nm grows with the loading of n-DMBI in the doped PNDI2TEG-2Tz film. These new spectral features are attributed to polaron-induced transitions,^[37] and can be considered as proof that the two D–A copolymers are doped.

Generally, the loss of the transitions in the neutral spectra is caused by the ICT or orbital hybridization between the host and dopant molecules, which generates CTC. Figure 3c shows the relative neutral peak intensities of differently doped D–A copolymers, which are normalized to those of their pristine films. Interestingly, the normalized neutral peak intensity scales linearly with the doping concentration for both D–A copolymers. This is consistent with their good host/dopant miscibilities as any phase-separation would render this sublinear. The formation efficiency (η_{CTC}) of the CTC during molecular doping can be estimated from the slopes in Figure 3c, which yields η_{CTC} of 38% and 47% for PNDI2TEG-2T and PNDI2TEG-2Tz, respectively. It is to be noted that the sign switching of Seebeck coefficient occurs at approximately 35 mol% for the doped PNDI2TEG-2T, corresponding to $\approx 13\%$ loss of the neutral band. This is very different from the work by Hwang et al. on chemically doped P(PymPh) where the neutral band is completely lost at the doping density that corresponds to a change in sign of the Seebeck coefficient.^[46]

As explained in the introduction, the formation of CTC states is only the first step towards free charge carriers. To determine the doping levels of both doped D–A copolymers, we directly measured the carrier density by using admittance spectroscopy on ion-gel-based metal–insulator–semiconductor (MIS) devices (see Figure S12, Supporting Information). The effectiveness of this strategy for the measurement of carrier density in moderately doped OSCs has been demonstrated previously.^[38] Figure 3d displays the carrier densities and doping efficiencies of doped PNDI2TEG-2T and PNDI2TEG-2Tz films.

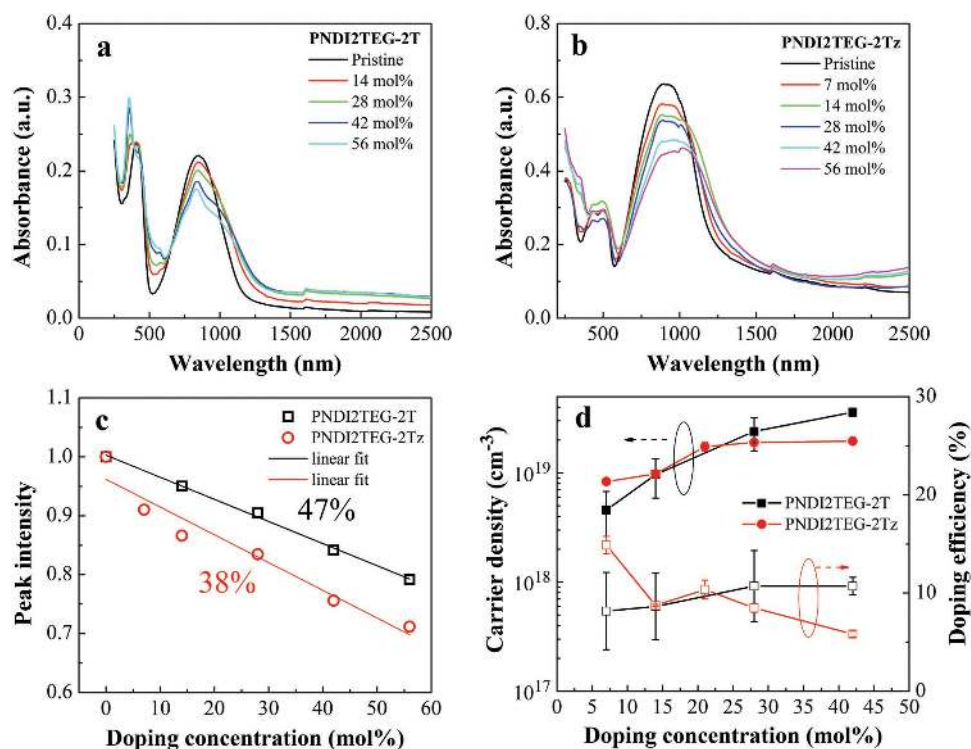


Figure 3. a,b) The UV-vis-NIR absorption spectra of pristine and doped PNDI2TEG-2T (a) and PNDI2TEG-2Tz (b); c) the absorption intensity at the neutral peak (843 nm for PNDI2TEG-2T and 907 nm for PNDI2TEG-2Tz) normalized to that of the pristine samples; d) the carrier densities extracted from MIS devices based on ion-gel dielectric layers and corresponding doping efficiencies as a function of the doping concentration in doped PNDI2TEG-2T and PNDI2TEG-2Tz films. A total DOS of $8 \times 10^{20} \text{ cm}^{-3}$ is used for both D-A copolymers.

The two doped D-A copolymers show similar carrier densities falling between 4×10^{18} to $4 \times 10^{19} \text{ cm}^{-3}$ at doping concentrations ranging from 7 mol% to 42 mol%, which gives a similar doping efficiency (η) of $\approx 10\%$ for both systems. These results indicate that the two D-A copolymers are similarly doped, i.e., the density of free carriers is similar. The sign of the Seebeck coefficient for PNDI2TEG-2T switches at a doping level of only 0.04, which is much lower than the required doping level of >1 according to the previous work.^[46] Given such a moderate doping level, it is unlikely the E_F will pass over the level of the pristine conduction band to cause the sign switching of the Seebeck coefficient for doped PNDI2TEG-2T.

The similar and moderate doping levels of the two doped D-A copolymers could not explain their huge difference in electrical conductivity and the unusual sign switching of the Seebeck coefficient in the doped PNDI2TEG-2T. To explore the underlying reasons, we directly measured the DOS functions for both D-A copolymers using an electrochemical method (see Figures S13 and S14, Supporting Information). Different from previous reports,^[47,48] we use an ion liquid as the electrolyte instead of organic solvent/inorganic salts for the purpose of keeping the organic films from being partially dissolved. Figure 4 displays the measured DOS energy distributions versus the Ag reference for the pristine PNDI2TEG-2T (open black symbols) and PNDI2TEG-2Tz (open red symbols). Clearly, the PNDI2TEG-2Tz film exhibits a DOS distribution not only with higher site density than that of PNDI2TEG-2T but also with narrower distribution. We attribute the changes of

DOS distribution to the improved backbone planarity and structural order in the in-plane direction after tailoring the donor moiety. The mobility measurement of pristine D-A copolymers by field-effect transistor with a bottom gate/bottom contact geometry shows three orders of magnitude enhancement of mobility after backbone modification (from 9.3×10^{-7} to

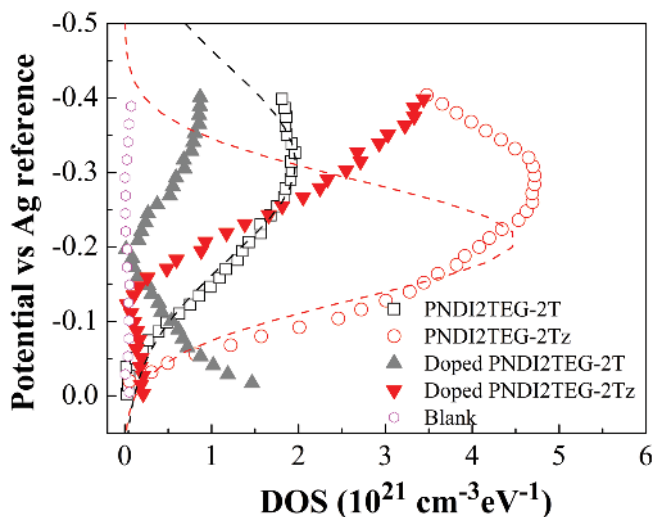


Figure 4. The measured DOS functions of PNDI2TEG-2T and PNDI2TEG-2Tz in the pristine (open symbols) and 28 mol%-doped state (closed symbols). The dashed lines are Gaussian fits.

$1.2 \times 10^{-3} \text{ cm}^2 \text{ Vs}^{-1}$, see Figure S15, Supporting Information). This agrees with the difference between the DOS distributions of two D–A copolymers. The first half of DOS distribution in the two D–A copolymers, which is mostly relevant to the charge transport, can be well approximated by the Gaussian function (the dash lines).

$$g(E) = \frac{N_m}{\sqrt{2\pi}\sigma_d} \exp\left[-\left(\frac{E-E_{ct}}{\sqrt{2}\sigma_d}\right)^2\right] \quad (2)$$

The total density N_m of 6.4×10^{20} and $8.8 \times 10^{20} \text{ cm}^{-3}$, E_{ct} of -0.31 and -0.21 eV , and the width σ_d of 130 and 78 meV are obtained for the PNDI2TEG-2T and PNDI2TEG-2Tz, respectively. Upon molecular doping with 28 mol% n-DMBI, the original neutral DOS are reduced and shifted upwards for both D–A copolymers. Interestingly, another newly formed energy band sitting below the neutral band was observed in the doped PNDI2TEG-2T. We assigned these new states to CTCs. However, such a CTC band was not seen in the doped PNDI2TEG-2Tz. It should be pointed out that does not mean that there are no CTC states in the doped PNDI2TEG-2Tz. We believe that the CTC states exist in the doped PNDI2TEG-2Tz, as its neutral band is actually lost upon doping, but the ΔE is too small to make a CTC band resolvable. The underlying reason is not clear at this stage. We speculate it might be related to the carrier delocalization, which is highly impacted by molecular planarity and structural order. These results indicate that the modification of donor moiety by introducing $\text{sp}^2\text{-N}$ atoms changes not only the DOS distribution in the pristine state but also that in the doped state. The narrower and denser DOS distribution of PNDI2TEG-2Tz as compared with that of PNDI2TEG-2T largely contributed to the huge enhancement of electrical conductivity.^[49,50]

Besides the introduction of $\text{sp}^2\text{-N}$ atoms, PNDI2TEG-2Tz and PNDI2TEG-2T also differ in molecular weight ($M_W = 30 \text{ kg mol}^{-1}$ for the former versus $M_W = 14 \text{ kg mol}^{-1}$ for the latter). In general, the molecular weight can affect the microstructure of the doped polymer and the mobility of charge carriers. However, the effects of the molecular weight on the properties of the doped films are not easily intuited. In the pristine state, a sufficiently low molecular weight reduces the mobility because higher molecular weights tend to lead to higher degrees of crystallinity (i.e., π -stacking). However, highly crystalline polymers can also drive phase-segregation when doped, leading to poor morphologies and low doping efficiencies. Recent studies by Müller and coworkers show that the molecular weight has little influence on the electrical conductivity of n-doped and p-doped polymers.^[28,51] We have measured the conductivity and Seebeck coefficient of the hexane-fraction (i.e., low molecular weight) of PNDI2TEG-2T in the doped state (see Figure S16, Supporting Information). The performance of this low-molecular-weight fraction is very similar to that shown in Figure 2, suggesting that the molecular weight does not significantly influence the results. We therefore tentatively conclude that the difference in power factor and conductivity between PNDI2TEG-2T and PNDI2TEG-2Tz is not caused by the difference in molecular weight.

How to explain the change of sign of the Seebeck coefficient in moderately doped PNDI2TEG-2T? To get some

insights, we rewrite Equation (1) in terms of the transport energy E_T as

$$S = -\frac{1}{qT} (E_T - E_F), \quad (3)$$

where the transport energy is defined as

$$E_T = \int E \frac{\sigma(E)}{\sigma} dE \quad (4)$$

As implied by Equation (3), the sign of the Seebeck coefficient is determined by the relative positions of the E_F and the E_T . If a Gaussian DOS is filled such that the E_F sits below the center of the DOS, the Seebeck coefficient is negative (n-type doping, see the left-hand panel in Figure 5a). As the doping level increases, the E_F overtakes the E_T and the sign of the Seebeck coefficient changes (the middle panel in Figure 5a). This only occurs at very high doping densities, as reported by Hwang et al.^[46] As previously mentioned, it is not possible that the E_F crosses the original LUMO level at a moderate doping level in doped PNDI2TEG-2T. However, the DOS of doped PNDI2TEG-2T is not a single Gaussian (like the case indicated by the right-hand panel in Figure 5a) as it contains CTC states. The thermal ionization of CTC states generates not only free electrons in the neutral band, but also the same amount of holes on CTC sites.^[16] As a result, carriers can also hop between CTC states.^[16] Such hopping between CTC states, however, occurs below the Fermi energy, and thus has a contribution to the Seebeck coefficient that is positive in sign. The Seebeck coefficient will then be the result of hopping between CTC states and hopping in the neutral band. If charge transport through the host itself is poor (as is the case for PNDI2TEG-2T), the Seebeck coefficient can even change sign as a result. To illustrate this, we performed numerical simulations by taking account of the CTC states (details can be found in the Supporting Information). No attempt at obtaining quantitative agreement was made as we are aiming for a qualitative description of the experimental findings. In this model, we consider that the total DOS of a doped film results from a superposition of two Gaussian-shaped DOS functions of neutral states (host) and CTC states. The two DOS distributions are energetically separated from each other by ΔE . The jump from one site to another (host or CTC state) is governed by the extent of localization. We define the factor β as the ratio of the two inverse localisation lengths, i.e., $\beta = \alpha_{\text{host}}/\alpha_{\text{CTC}}$. If β is unity, then CTC states and the host are equally conductive. If, on the other hand, β is larger than unity then CTC states will be more conductive than the host.

Figure 5b demonstrates the scenario of $\Delta E = 0.4 \text{ meV}$ and CTC fraction = 36% (the top panel). The simulation shows that the charge transport energy (E_T), at moderate doping, moves from above the Fermi energy to below it even by slightly changing β from 1 to 1.25. As a result, the Seebeck coefficient changes sign from negative to positive at doping densities that are too small to allow the E_F to cross the LUMO. A fundamental insight we gained from the numerical simulation is that a sign switching of S may only be seen in a moderately doped organic system when enough CTC states are below the E_F and

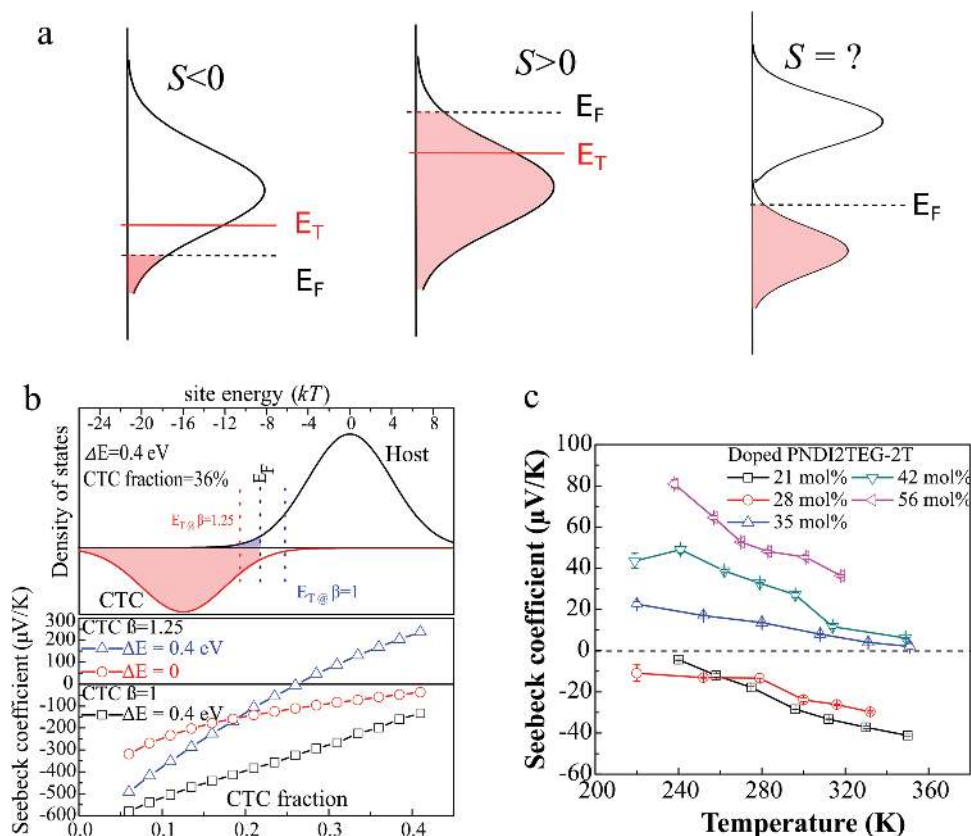


Figure 5. a) If a Gaussian DOS is filled at moderate n-doping, E_T is above the E_F , and $S < 0$ (the left-hand panel); however, in the case of very high n-doping level, the positions of the E_T and E_F reverse, which results in $S > 0$ (the middle panel); and if the DOS is not a Gaussian, but contains multiple local maxima, the E_T can be above or below the E_F depending on the details of the DOS and the hopping mechanism (the right-hand panel). b) Numerical simulation results assuming Gaussian-shaped DOS for neutral (host) and CTC (guest) states: E_F and E_T position in the scenario of $\Delta E = 0.4$ eV and CTC fraction = 36% with $\beta = 1$ or $\beta = 1.25$ (the top panel), and the simulated Seebeck coefficient as a function of CTC fraction under conditions: $\Delta E = 0.4$ eV or 0 and $\beta = 1$ or 1.25 (the bottom panel); and c) the measured variable temperature Seebeck coefficient in differently doped PNDI2TEG-2T films.

the charges on the host states are more localized than those on CTC states. PNDI2TEG-2T appears to meet these criteria as it shows a very poor transport in the pristine state and CTC states below the neutral band after doping. As such, the unusual sign switching of S was observed in doped PNDI2TEG-2T. On the other hand, PNDI2TEG-2Tz exhibits much better charge transport in the neutral band, which may explain the absence of sign switching of the Seebeck coefficient in this system.

Presently, the charge transport through CTC states is poorly understood and more research efforts are required in this direction. However, we can modulate the magnitude of the conduction in the neutral band by changing the temperature as this process is known to be thermally activated.^[28,38,49] Figure 5c displays the variable temperature Seebeck coefficient in the doped PNDI2TEG-2T. By decreasing the temperature, we observed that the absolute values of negative Seebeck coefficients decrease while those of the positive Seebeck coefficients increase. These results can only be explained by taking account of charge conduction through CTC states. As the temperature drops, the neutral band conduction is suppressed and the conduction through CTC states becomes more significant and shifts the Seebeck coefficient towards the positive direction. We would like to emphasize that, even in a doped system without sign switching of S , conduction through CTC states still serves

as a leakage pathway for the Seebeck coefficient and conductivity. This is predicted by our simulated results (see Figure S17, Supporting Information). Our work highlights the importance of tailoring DOS for boosting the power factor by simultaneously increasing conductivity and Seebeck coefficient.

In summary, we demonstrated that the n-type thermoelectric performance of D–A copolymers can be greatly improved by tailoring the DOS distribution through molecular design. Here, the molecular design is embedding sp^2 -N atoms into the donor moiety of an NDI-2T based D–A copolymer (PNDI2TEG-2T). By doing so, a new copolymer named PNDI2TEG-2Tz with improved molecular planarity and the π - π overlap was obtained. Furthermore, the molecular stacking in the thin film is changed into a preferential edge-on pattern from the original face-on-dominated microstructure. Due to the molecular and microstructural motif, the PNDI2TEG-2Tz exhibits much narrower and denser DOS energy distribution than PNDI2TEG-2T. For this reason, the doped PNDI2TEG-2Tz copolymer exhibits a high electrical conductivity of 1.8 S cm^{-1} , which represents over three orders of magnitude enhancement as compared to that of unmodified D–A copolymer. Additionally, the tailoring of DOS distribution reduces the loss of the Seebeck coefficient, leading to an improved power factor of $4.5 \text{ } \mu\text{W m}^{-1} \text{ K}^{-2}$, which is a very good result for n-type OTE. Our

work provides insights into the fundamental understanding of the molecular doping and sheds light on designing efficient n-type OTE materials from a new perspective of tailoring the DOS.

Supporting Information

Supporting Information is available from the Wiley Online Library or from the author.

Acknowledgements

J.L. and G.Y. contributed equally to this work. This work is part of the research programme of the Foundation of Fundamental Research on Matter (FOM), which is part of the Netherlands Organisation for Scientific Research (NWO). This is a publication by the FOM Focus Group 'Next Generation Organic Photovoltaics', participating in the Dutch Institute for Fundamental Energy Research (DIFFER). G.Y., J. D., and Y. L. acknowledge financial support from the China Scholarship Council. J. L. thanks Matt. P. Garman and Marten Koopmans for useful discussion. We would like to greatly thank Dr. Jianhua Chen and Prof. Dr. Xugang Guo from South University of Science and Technology of China (SUSTC) for GPC measurement.

Conflict of Interest

The authors declare no conflict of interest.

Keywords

donor–acceptor copolymers, electrical conductivity and density of states, n-type doping, solution processing

Received: July 6, 2018

Revised: August 1, 2018

Published online: September 17, 2018

- [1] P. Pingel, D. Neher, *Phys. Rev. B* **2013**, *87*, 115209.
- [2] I. Salzmänn, G. Heimel, S. Duhm, M. Oehzelt, P. Pingel, B. M. George, A. Schnegg, K. Lips, R.-P. Blum, A. Vollmer, N. Koch, *Phys. Rev. Lett.* **2012**, *108*, 035502.
- [3] C.-Z. Li, C.-C. Chueh, H.-L. Yip, F. Ding, X. Li, A. K.-Y. Jen, *Adv. Mater.* **2013**, *25*, 2457.
- [4] X. Lin, B. Wegner, K. M. Lee, M. A. Fusella, F. Zhang, K. Moudgil, B. P. Rand, S. Barlow, S. R. Marder, N. Koch, A. Kahn, *Nat. Mater.* **2017**, *16*, 1209.
- [5] B. Lüssem, M. Riede, K. Leo, *Phys. Status solidi* **2013**, *210*, 9.
- [6] W. Shi, J. Chen, J. Xi, D. Wang, Z. Shuai, *Chem. Mater.* **2014**, *26*, 2669.
- [7] M. L. Tietze, P. Pöhner, K. Schmidt, K. Leo, B. Lüssem, *Adv. Funct. Mater.* **2015**, *25*, 2701.
- [8] S. Wang, H. Sun, U. Ail, M. Vagin, P. O. Å. Persson, J. W. Andreasen, W. Thiel, M. Berggren, X. Crispin, D. Fazzi, S. Fabiano, *Adv. Mater.* **2016**, *28*, 10764.
- [9] Y. Xuan, X. Liu, S. Desbief, P. Leclère, M. Fahlman, R. Lazzaroni, M. Berggren, J. Cornil, D. Emin, X. Crispin, *Phys. Rev. B* **2010**, *82*, 115454.
- [10] I. Salzmänn, G. Heimel, M. Oehzelt, S. Winkler, N. Koch, *Acc. Chem. Res.* **2016**, *49*, 370.
- [11] M. Culebras, C. Gómez, A. Cantarero, *Materials (Basel)*. **2014**, *7*, 6701.
- [12] A. A. Günther, M. Sawatzki, P. Formánek, D. Kasemann, K. Leo, *Adv. Funct. Mater.* **2016**, *26*, 768.
- [13] J. T. E. Quinn, J. Zhu, X. Li, J. Wang, Y. Li, *J. Mater. Chem. C* **2017**, *5*, 8654.
- [14] K. S. Yook, S. O. Jeon, S.-Y. Min, J. Y. Lee, H.-J. Yang, T. Noh, S.-K. Kang, T.-W. Lee, *Adv. Funct. Mater.* **2010**, *20*, 1797.
- [15] H. Méndez, G. Heimel, S. Winkler, J. Frisch, A. Opitz, K. Sauer, B. Wegner, M. Oehzelt, C. Röthel, S. Duhm, D. Többsens, N. Koch, I. Salzmänn, *Nat. Commun.* **2015**, *6*, 8560.
- [16] M. L. Tietze, J. Benduhn, P. Pöhner, B. Nell, M. Schwarze, H. Kleemann, M. Krammer, K. Zojer, K. Vandewal, K. Leo, *Nat. Commun.* **2018**, *9*, 1182.
- [17] J.-M. Kim, S.-J. Yoo, C.-K. Moon, B. Sim, J.-H. Lee, H. Lim, J. W. Kim, J.-J. Kim, *J. Phys. Chem. C* **2016**, *120*, 9475.
- [18] M. Oehzelt, N. Koch, G. Heimel, *Nat. Commun.* **2014**, *5*, 4174.
- [19] O. Bubnova, Z. U. Khan, A. Malti, S. Braun, M. Fahlman, M. Berggren, X. Crispin, *Nat. Mater.* **2011**, *10*, 429.
- [20] N. Lu, L. Li, M. Liu, *Phys. Chem. Chem. Phys.* **2016**, *18*, 19503.
- [21] J. Yang, H.-L. Yip, A. K.-Y. Jen, *Adv. Energy Mater.* **2013**, *3*, 549.
- [22] G.-H. Kim, L. Shao, K. Zhang, K. P. Pipe, *Nat. Mater.* **2013**, *12*, 719.
- [23] D. Huang, H. Yao, Y. Cui, Y. Zou, F. Zhang, C. Wang, H. Shen, W. Jin, J. Zhu, Y. Diao, W. Xu, C. A. Di, D. Zhu, *J. Am. Chem. Soc.* **2017**, *139*, 13013.
- [24] Y. Wang, M. Nakano, T. Michinobu, Y. Kiyota, T. Mori, K. Takimiya, *Macromolecules* **2017**, *50*, 857.
- [25] W. Ma, K. Shi, Y. Wu, Z.-Y. Lu, H.-Y. Liu, J.-Y. Wang, J. Pei, *ACS Appl. Mater. Interfaces* **2016**, *8*, 24737.
- [26] L. Qiu, J. Liu, R. Alessandri, X. Qiu, M. Koopmans, R. W. A. Havenith, S. J. Marrink, R. C. Chiechi, L. J. Anton Koster, J. C. Hummelen, *J. Mater. Chem. A* **2017**, *5*, 21234.
- [27] J. Liu, L. Qiu, G. Portale, M. Koopmans, G. ten Brink, J. C. Hummelen, L. J. A. Koster, *Adv. Mater.* **2017**, *29*, 1701641.
- [28] D. Kiefer, A. Giovannitti, H. Sun, T. Biskup, A. Hofmann, M. Koopmans, C. Cendra, S. Weber, L. J. Anton Koster, E. Olsson, J. Rivnay, S. Fabiano, I. McCulloch, C. Müller, *ACS Energy Lett.* **2018**, *3*, 278.
- [29] X. Zhao, D. Madan, Y. Cheng, J. Zhou, H. Li, S. M. Thon, A. E. Bragg, M. E. DeCoster, P. E. Hopkins, H. E. Katz, *Adv. Mater.* **2017**, *29*, 1606928.
- [30] E. E. Perry, C.-Y. Chiu, K. Moudgil, R. A. Schlitz, C. J. Takacs, K. A. O'Hara, J. G. Labram, A. M. Glauddell, J. B. Sherman, S. Barlow, C. J. Hawker, S. R. Marder, M. L. Chabinyc, *Chem. Mater.* **2017**, *29*, 9742.
- [31] K. Shi, F. Zhang, C.-A. Di, T.-W. Yan, Y. Zou, X. Zhou, D. Zhu, J.-Y. Wang, J. Pei, *J. Am. Chem. Soc.* **2015**, *137*, 6979.
- [32] Y. Shin, M. Massetti, H. Komber, T. Biskup, D. Nava, G. Lanzani, M. Caironi, M. Sommer, *Adv. Electron. Mater.* **2018**, <https://doi.org/10.1002/aelm.201700581>.
- [33] S. Wang, H. Sun, T. Erdmann, G. Wang, D. Fazzi, U. Lappan, Y. Püttisong, Z. Chen, M. Berggren, X. Crispin, A. Kiriy, B. Voit, T. J. Marks, S. Fabiano, A. Facchetti, **2018**, *1801898*, 1.
- [34] H. Yan, Z. Chen, Y. Zheng, C. Newman, J. R. Quinn, F. Döt, M. Kastler, A. Facchetti, *Nature* **2009**, *457*, 679.
- [35] M. Li, C. An, W. Pisula, K. Müllen, *Acc. Chem. Res.* **2018**, *51*, 1196.
- [36] R. A. Schlitz, F. G. Brunetti, A. M. Glauddell, P. L. Miller, M. A. Brady, C. J. Takacs, C. J. Hawker, M. L. Chabinyc, *Adv. Mater.* **2014**, *26*, 2825.
- [37] B. D. Naab, X. Gu, T. Kurosawa, J. W. F. To, A. Salleo, Z. Bao, *Adv. Electron. Mater.* **2016**, *2*, 1600004.

- [38] J. Liu, L. Qiu, R. Alessandri, X. Qiu, G. Portale, J. Dong, W. Talsma, G. Ye, A. A. Sengrian, P. C. T. Souza, M. A. Loi, R. C. Chiechi, S. J. Marrink, J. C. Hummelen, L. J. A. Koster, *Adv. Mater.* **2018**, *30*, 1704630.
- [39] H. Fritzsche, *Solid State Commun.* **1971**, *9*, 1813.
- [40] G. Zuo, X. Liu, M. Fahlman, M. Kemerink, *Adv. Funct. Mater.* **2018**, *28*, 1703280.
- [41] Y.-Z. Dai, N. Ai, Y. Lu, Y.-Q. Zheng, J.-H. Dou, K. Shi, T. Lei, J.-Y. Wang, J. Pei, *Chem. Sci.* **2016**, *7*, 5753.
- [42] C. Gaul, S. Hutsch, M. Schwarze, K. S. Schellhammer, F. Bussolotti, S. Kera, G. Cuniberti, K. Leo, F. Ortman, *Nat. Mater.* **2018**, *17*, 439.
- [43] J. Rivnay, M. F. Toney, Y. Zheng, I. V. Kauvar, Z. Chen, V. Wagner, A. Facchetti, A. Salleo, *Adv. Mater.* **2010**, *22*, 4359.
- [44] Y. Shi, H. Guo, M. Qin, J. Zhao, Y. Wang, H. Wang, Y. Wang, A. Facchetti, X. Lu, X. Guo, *Adv. Mater.* **2018**, *30*, 1705745.
- [45] H. Wang, U. Ail, R. Gabrielsson, M. Berggren, X. Crispin, *Adv. Energy Mater.* **2015**, *5*, 1500044.
- [46] S. Hwang, W. J. Potscavage, Y. S. Yang, I. S. Park, T. Matsushima, C. Adachi, Y. Q. Li, J. X. Tang, S. R. Marder, Z. Bao, W. Xu, D. Zhu, Y. Gao, Y. Cui, Z. Bao, *Phys. Chem. Chem. Phys.* **2016**, *18*, 29199.
- [47] I. N. Hulea, H. B. Brom, A. J. Houtepen, D. Vanmaekelbergh, J. J. Kelly, E. A. Meulenkaamp, *Phys. Rev. Lett.* **2004**, *93*, 16.
- [48] J. Bisquert, F. Fabregat-Santiago, I. Mora-Seró, G. Garcia-Belmonte, E. M. Barea, E. Palomares, *Inorg. Chim. Acta* **2008**, *361*, 684.
- [49] W. F. Pasveer, J. Cottaar, C. Tanase, R. Coehoorn, P. A. Bobbert, P. W. M. Blom, D. M. de Leeuw, M. A. J. Michels, *Phys. Rev. Lett.* **2005**, *94*, 206601.
- [50] R. Coehoorn, W. F. Pasveer, P. A. Bobbert, M. A. J. Michels, *Phys. Rev. B* **2005**, *72*, 155206.
- [51] J. Hynynen, D. Kiefer, L. Yu, R. Kroon, R. Munir, A. Amassian, M. Kemerink, C. Müller, *Macromolecules* **2017**, *50*, 8140.